Available online at www.sciencedirect.com
ScienceDirect
International Journal of Heat and Mass Transfer 50 (2007) 2634–2642
International Journal of HEAT and MASS TRANSFER
www.elsevier.com/locate/ijhmt

Solution of radiative heat transfer in graded index media by least square spectral element method

J.M. Zhao, L.H. Liu *

School of Energy Science and Engineering, Harbin Institute of Technology, 92 West Dazhi Street, Harbin 150001, People's Republic of China

Received 22 February 2006; received in revised form 26 September 2006
Available online 20 February 2007

Abstract

Least square spectral element method based on discrete-ordinates equation is extended to solve multidimensional radiative heat transfer problems in semitransparent graded index media. Chebyshev polynomial is employed as expansion set for the spectral element discretization. Five various test problems were taken as examples to verify the least square spectral element formulation for solving radiative heat transfer in semitransparent graded index media. The predicted distributions of temperature and radiative heat flux are determined by the least square spectral element method and compared with data in the references. The results show that the least square spectral element method has good accuracy for solving multidimensional radiative heat transfer problems in semitransparent graded index media.

Keywords: Radiative heat transfer; Graded index; Semitransparent media; Spectral element method

1. Introduction

Due to the structural characteristics of a material or a possible temperature dependency, the refractive index of a media may be a function of spatial position. The radiative heat transfer in semitransparent media with graded index is of great interest in thermo-optical systems, and has evoked the wide interest of many researchers. In graded index media, the ray goes along a curved path determined by the Fermat principle. As a result, the solution of radiative transfer in a graded index media is more difficult than that in a uniform index media. Curved ray-tracing technique was developed and widely used to solve this kind of problem, such as, the ray-tracing techniques presented by Abdallah and coworkers [1–3], Huang et al. [4,5], and Liu and coworkers [6,7]. For the radiative transfer problems in multidimensional graded index media, the curved ray tracing is very difficult and complex, and hence the methods based on the curved ray-tracing techniques were mainly limited to one-dimensional radiative transfer problems. Recently, to avoid the complicated computation of curved ray trajectories, Liu [8] deduced the three-dimensional radiative transfer equation within graded index media in Cartesian coordinate system and developed a finite volume method (FVM) for solving multidimensional radiative transfer problems in graded index media. Based on the radiative transfer equation deduced in Ref. [8], Liu and coworkers [9] developed the finite element method (FEM) for multidimensional graded index media. These non-ray-tracing methods avoid the complicated and time-consuming computation of curved ray trajectory and can be easily used to solve multidimensional problems. However, these methods just offer *h*-convergence, i.e. the convergence gained by reducing the element size *h* or *h*-refinement, as a result, re-meshing or refining have to be done in order to gain the wanted accuracy.

Spectral element approximation, originally proposed by Patera [10] for the solution of fluid problem, combines the advantages of spectral approximation with *p*-convergence and finite element approximation with *h*-convergence and the flexibility to deal with complex domain. The *p*-convergence of spectral element approximation makes it more

* Corresponding author. Tel.: +86 451 86402237; fax: +86 451 86221048.
E-mail address: lhliu@hit.edu.cn (L.H. Liu).

0017-9310/$ - see front matter © 2007 Elsevier Ltd. All rights reserved.
doi:10.1016/j.ijheatmasstransfer.2006.11.032

Nomenclature

h	element size, Lagrange interpolation polynomial defined in Eq. (13)
$\mathbf{H}$	matrix defined in Eq. (22)
I	radiative intensity
I_b	blackbody radiative intensity
$\widetilde{I}$	approximate radiative intensity
$\mathbf{i},\mathbf{j},\mathbf{k}$	unit vectors into the x-, y- and z-directions, respectively
L	slab thickness, side length of rectangular media
$\mathbf{n}$	inward normal vector
n	refractive index
N_{el}	total number of elements
N_{esol}	number of solution nodes per element
N_{sol}	total number of solution nodes
p	polynomial order
q	radiative heat flux (W/m^2)
$\mathbf{r}$	vector of spatial position
$\mathbf{s}_l$	vector defined as $\mathbf{s}_l = -\mathbf{i}\sin\varphi + \mathbf{j}\cos\varphi$
$\widetilde{S}$	variable defined in Eq. (7)
T	temperature (K)
T_g	media temperature (K)
V	solution domain
V_{st}	standard element
W	weight function
$\mathbf{x}$	cartesian coordinate vector defined in solution domain
x,y,z	cartesian coordinates defined in solution domain

Greek symbols

$\tilde{\beta}$	variable defined in Eq. (7)
$\chi_\theta, \chi_\varphi$	variable defined by Eqs. (8) and (9), respectively
δ	variable defined in Eq. (14)
ε_w	wall emissivity
ϕ	global basis (shape function)
ϕ^e	elemental basis function defined on element e
Φ	scattering phase function
φ	azimuthal angle
$\Delta\varphi$	azimuthal angle step
κ_a	absorption coefficient (m^{-1})
κ_s	scattering coefficient (m^{-1})
$\mu^{m,n}, \xi^{m,n}, \eta^{m,n}$	direction cosine of the direction (m,n)
θ	polar angle
$\Delta\theta$	polar angle step
σ	Stefan–Boltzmann constant ($W/m^2\,K^4$)
τ_L	optical thickness, $\tau_L = (\kappa_a + \kappa_s)L$
$\mathbf{\Omega}, \mathbf{\Omega}'$	vector of radiation direction, $\mathbf{\Omega} = \mathbf{i}\mu + \mathbf{j}\eta + \mathbf{k}\xi$
Ω	solid angle
$\boldsymbol{\zeta}$	Cartesian coordinate vector defined in standard element
ζ,γ,ς	Cartesian coordinates defined in standard element
ω	single scattering albedo, $\omega = \kappa_s/(\kappa_a + \kappa_s)$
$\mathfrak{I}$	first-order linear differential operator defined in Eq. (20)
$\hbar$	two-dimensional spectral nodal basis defined on V_{st}^2
$\nabla, \nabla_{\mathbf{x}}$	gradient operator respect to $\mathbf{x}$, $\nabla_{\mathbf{x}} = \mathbf{i}\frac{\partial}{\partial x} + \mathbf{j}\frac{\partial}{\partial y} + \mathbf{k}\frac{\partial}{\partial z}$
∇_ζ	gradient operator respect to $\boldsymbol{\zeta}$, $\nabla_\zeta = \mathbf{i}\frac{\partial}{\partial \zeta} + \mathbf{j}\frac{\partial}{\partial \gamma} + \mathbf{k}\frac{\partial}{\partial \varsigma}$

Subscripts

e	element index
j,p	solution node index
w	value at wall boundary

Superscripts

1, 2	denote one- and two-dimensional, respectively
e	function defined on element e
$m, m', n, n', m \pm 1/2, n \pm 1/2$	angular direction of radiation

flexible and the solution accuracy be easily improved by just increasing the order or p-refinement of spectral approximation without refining or re-meshing the geometric mesh. As a result, spectral element approximation is more effective than spectral approximation and finite element approximation. Spectral element method has been successfully applied in computational fluid dynamics and heat transfer [10–14], and hence it's a natural idea to extend this method to solve radiative transfer problem. Recently, for radiative transfer within uniform index media, Pontaza and Reddy [15] proposed least square *hp* finite element formulations for solving one-dimensional radiative transfer equation (RTE). Considering RTE is a special case of the general convection-diffusion equation and the presence of convection term may cause non-physical oscillatory of solutions [16], Zhao and Liu [17] developed a least square spectral element method (LSSEM) for solving multidimensional radiative transfer problems in uniform index media.

In this paper, we extend the LSSEM approach to solve multidimensional radiative transfer problems in graded index media based on the discrete-ordinates equation. Five various test cases of radiative heat transfer in semitransparent media are taken to verify the performance of the method.

2. Mathematical formula

2.1. Discrete-ordinates equation of RTE

In the Cartesian coordinate system, radiative heat transfer equation in a multidimensional graded index media can be written as [8]

$$\boldsymbol{\Omega}\cdot\nabla I(\mathbf{r},\boldsymbol{\Omega})+\frac{1}{\sin\theta}\frac{\partial}{\partial\theta}\{[I(\mathbf{r},\boldsymbol{\Omega})(\xi\boldsymbol{\Omega}-\mathbf{k})]\}\cdot\frac{\nabla n}{n}+\frac{1}{\sin\theta}\frac{\partial}{\partial\varphi}\{I(\mathbf{r},\boldsymbol{\Omega})\mathbf{s}_1\}\cdot\frac{\nabla n}{n}+(\kappa_a+\kappa_s)I(\mathbf{r},\boldsymbol{\Omega})=n^2\kappa_a I_b(\mathbf{r})+\frac{\kappa_s}{4\pi}\int_{4\pi}I(\mathbf{r},\boldsymbol{\Omega}')\Phi(\boldsymbol{\Omega},\boldsymbol{\Omega}')\mathrm{d}\Omega'. \quad (1)$$

For the opaque, diffuse emitting and reflecting wall, boundary condition is given by

$$I(\mathbf{r}_w,\boldsymbol{\Omega})=n^2\varepsilon_w I_b(\mathbf{r}_w)+\frac{1-\varepsilon_w}{\pi}\int_{\mathbf{n}_w\cdot\boldsymbol{\Omega}'<0}I(\mathbf{r}_w,\boldsymbol{\Omega}')|\mathbf{n}_w\cdot\boldsymbol{\Omega}'|\mathrm{d}\Omega', \quad (2)$$

where $I(\mathbf{r},\boldsymbol{\Omega})$ is the radiative intensity, which is a function of spatial position $\mathbf{r}$ and direction $\boldsymbol{\Omega}=\mathbf{i}\mu+\mathbf{j}\eta+\mathbf{k}\xi$, μ, η, and ξ are the direction cosine of the local tangent vector of ray trajectory along the Cartesian coordinates x, y, and z directions, respectively, $I_b(\mathbf{r})$ is the blackbody radiative intensity at the temperature of the media, n is the refractive index of media, which is a function of spatial position, κ_a and κ_s are the absorption and the scattering coefficients, respectively, $\Phi(\boldsymbol{\Omega}',\boldsymbol{\Omega})$ is the scattering phase function from the incoming direction $\boldsymbol{\Omega}'$ to the outgoing direction $\boldsymbol{\Omega}$, θ and φ are the polar and the azimuthal angles, respectively, and $\mathbf{s}_1$ is the vector defined by $\mathbf{s}_1=-\mathbf{i}\sin\varphi+\mathbf{j}\cos\varphi$.

Eq. (1) differs from the radiative transfer equation in uniform index media. It contains two angular redistribution terms. For the discretization of the angular redistribution terms, piecewise constant angular (PCA) quadrature and step scheme is employed in Ref. [9]. In the PCA quadrature approach, the total solid angle is divided uniformly in the polar θ and azimuthal φ directions. In this paper, we use the same discretization method of angular redistribution terms employed in Ref. [9]. The discrete polar and azimuthal angles are discretized as follows:

$$\theta^m=(m-1/2)\Delta\theta,\quad m=1,2,\ldots,N_\theta, \quad (3a)$$

$$\varphi^n=(n-1/2)\Delta\varphi,\quad n=1,2,\ldots,N_\varphi, \quad (3b)$$

where $\Delta\theta=\pi/N_\theta$ and $\Delta\varphi=2\pi/N_\varphi$ are the steps for the discretization of polar and azimuthal angles, respectively, N_θ and N_φ correspondingly denote the numbers of divisions. For each discrete direction (m,n), the corresponding weight is

$$w_\theta^m=\cos\theta^{m-1/2}-\cos\theta^{m+1/2}, \quad (4a)$$

$$w_\varphi^n=\varphi^{n+1/2}-\varphi^{n-1/2}, \quad (4b)$$

where

$$\theta^{m+1/2}=(\theta^m+\theta^{m+1})/2, \quad (5a)$$

$$\varphi^{n+1/2}=(\varphi^n+\varphi^{n+1})/2. \quad (5b)$$

By using the PCA quadrature and step scheme for angular redistribution terms in Eq. (1), the discrete ordinates equation of radiative transfer for multidimensional problems in graded index media can be expressed as

$$\mu^{m,n}\frac{\partial I^{m,n}}{\partial x}+\eta^{m,n}\frac{\partial I^{m,n}}{\partial y}+\xi^{m,n}\frac{\partial I^{m,n}}{\partial z}+\tilde{\beta}^{m,n}(\mathbf{r})I^{m,n}=S^{m,n}(\mathbf{r}), \quad (6)$$

where

$$\tilde{\beta}^{m,n}(\mathbf{r})=\frac{1}{w_\theta^m}\max(\chi_\theta^{m+1/2,n},0)+\frac{1}{w_\theta^m}\max(-\chi_\theta^{m-1/2,n},0)+\frac{1}{w_\varphi^n}\max(\chi_\varphi^{m,n+1/2},0)+\frac{1}{w_\varphi^n}\max(-\chi_\varphi^{m,n-1/2},0)+(\kappa_a+\kappa_s), \quad (7a)$$

$$\tilde{S}^{m,n}(\mathbf{r})=n^2\kappa_a I_b+\frac{\kappa_s}{4\pi}\sum_{m'=1}^{N_\theta}\sum_{n'=1}^{N_\varphi}I^{m',n'}\Phi^{m',n';m,n}w_\theta^{m'}w_\varphi^{n'}+\frac{1}{w_\theta^m}\max(-\chi_\theta^{m+1/2,n},0)I^{m+1,n}+\frac{1}{w_\theta^m}\max(\chi_\theta^{m-1/2,n},0)I^{m-1,n}+\frac{1}{w_\varphi^n}\max(-\chi_\varphi^{m,n+1/2},0)I^{m,n+1}+\frac{1}{w_\varphi^n}\max(\chi_\varphi^{m,n-1/2},0)I^{m,n-1}. \quad (7b)$$

The recursion formula for $\chi_\theta^{m+1/2,n}$ and $\chi_\varphi^{m,n+1/2}$ are giving as following [9]:

$$\chi_\theta^{m+1/2,n}-\chi_\theta^{m-1/2,n}=\frac{w_\theta^m}{\sin\theta^m}\left[\frac{\partial(\xi\boldsymbol{\Omega})}{\partial\theta}\cdot\frac{\nabla n}{n}\right]_{\Omega=\Omega^{m,n}}, \quad (8a)$$

$$\chi_\theta^{1/2,n}=\chi_\theta^{N_\theta+1/2,n}=0, \quad (8b)$$

$$\chi_\varphi^{m,n+1/2}-\chi_\varphi^{m,n-1/2}=\frac{w_\varphi^n}{\sin\theta^m}\left[\frac{\partial\mathbf{s}_1}{\partial\varphi}\cdot\frac{\nabla n}{n}\right]_{\Omega=\Omega^{m,n}}, \quad (9a)$$

$$\chi_\varphi^{m,1/2}=\chi_\varphi^{m,N_\varphi+1/2}=\frac{1}{\sin\theta^m}\left(\mathbf{j}\cdot\frac{\nabla n}{n}\right). \quad (9b)$$

Eq. (6) with boundary condition given by Eq. (2) is solved for each discrete direction. It can be seen that both $\tilde{\beta}^{m,n}(\mathbf{r})$ and $S^{m,n}(\mathbf{r})$ contain part of angular redistribution terms, this is different from the discrete-ordinates equation of radiative transfer in uniform media. Therefore, source term updating is always needed during the solution process.

2.2. Spectral element approximation

Spectral element approximation combines the advantages of spectral approximation with p-convergence and finite element approximation with h-convergence. In spectral element approximation, the solution domain V is decomposed into N_{el} non-overlapping elements V_e, and any function defined over the solution domain is approximated by its spectral expansion over each element. The spectral basis are originally defined on standard element V_{st} and transformed to each general element V_e to build elemental basis functions ϕ_i^e over V_e. With Lagrange nodal basis expansion, the spectral element approximation can be formulated in a form as in finite element approximation. Considering the elemental nodal basis as shape function, the radiative intensity can be approximated over element V_e by

$$\widetilde{I}^{m,n,e}(\mathbf{x})=\sum_{i=1}^{N_{esol}}I_i^{m,n,e}\phi_i^e(\mathbf{x}) \quad (10)$$

where $I_i^{m,n,e}$ denotes the radiative intensity at the ith node of element V_e, $\phi_i^e(\mathbf{r})$ is Lagrange nodal basis function defined on element V_e, and N_{esol} denotes the number of solution nodes per element.

Using globally assemble procedure as in finite element method, nodal basis functions on each element around node j can be assembled as the global basis of node j, denoted by ϕ_j. The globally approximation intensity $\widetilde{I}^{m,n}$ can be written as

$$\widetilde{I}^{m,n}(\mathbf{x}) = \sum_{j=1}^{N_{\mathrm{sol}}} I_j^{m,n}\phi_j(\mathbf{x}), \tag{11}$$

where $I_j^{m,n}$ denotes the radiative intensity at solution node j and N_{sol} is the total number of solution nodes over the solution domain.

Chebyshev and Legendre polynomials are two most commonly used expansion sets in spectral element method for non-periodical problems. In this paper, Chebyshev polynomial is employed to build the elemental nodal basis functions. The $N-1$ order nodal basis functions defined on standard element $V_{\mathrm{st}}^1 = [-1,1]$ are Lagrange interpolation polynomials through N Chebyshev–Gauss–Lobatto points:

$$\zeta_j = -\cos\left(\frac{j-1}{N-1}\pi\right), \quad j = 1,\ldots,N. \tag{12}$$

By using barycentric interpolation formula, the Lagrange interpolation polynomials can be written as [18]

$$h_i(\zeta) = \frac{\frac{w_i}{\zeta-\zeta_i}}{\sum_{j=1}^{N}\frac{w_j}{\zeta-\zeta_j}}, \tag{13}$$

where

$$w_j = (-1)^{j-1}\delta_j, \quad \delta_j = \begin{cases} 1/2, & j = 1 \text{ or } j = N, \\ 1, & \text{otherwise.} \end{cases} \tag{14}$$

The barycentric interpolation formula is considered to be accurate and more computationally stable. This is demonstrated in Ref. [18–20].

Multidimensional spectral nodal basis function can be built with tensor product of the one-dimensional spectral nodal basis function $h_i(\zeta)$. For example, two-dimensional spectral nodal basis function $\hbar_{m(i,j)}$ defined on standard element $V_{\mathrm{st}}^2 = [-1,1]\times[-1,1]$ are given by

$$\hbar_{m(i,j)}(\zeta,\gamma) = h_i(\zeta)h_j(\gamma), \quad i,j = 1,\ldots,N, \tag{15}$$

where $m(i,j)$ is a index map function defined as

$$m = m(i,j) = (j-1)N + i, \tag{16}$$

which gives a index map from two-dimensional index to one-dimensional index, thus makes the formulation described above coherent for both one- and two-dimensional cases. Similar index map can be defined for three-dimensional case. The nodal basis defined on general element V_{e}^2 and on standard element V_{st}^2 are related by

$$\phi^{\mathrm{e}}_{m(i,j)}(\mathbf{x}(\boldsymbol{\zeta})) = \hbar^{\mathrm{e}}_{m(i,j)}(\boldsymbol{\zeta}), \quad \mathbf{x}\in\Omega_{\mathrm{e}}, \boldsymbol{\zeta}\in V_{\mathrm{st}}, \tag{17}$$

and with derivative relation:

$$\nabla_{\mathbf{x}}\phi^{\mathrm{e}}_{m(i,j)}(\mathbf{x}(\boldsymbol{\zeta})) = \mathbf{J}^{-1}\nabla_{\boldsymbol{\zeta}}\hbar^{\mathrm{e}}_{m(i,j)}(\boldsymbol{\zeta}), \tag{18}$$

where $\mathbf{x} = \mathbf{x}(\boldsymbol{\zeta})$ defines the coordinate transform from V_{st}^2 to V_{e}^2, $\nabla_{\mathbf{x}}$ and $\nabla_{\boldsymbol{\zeta}}$ are the gradient operator respect to $\mathbf{x}$ and $\boldsymbol{\zeta}$, respectively, and $\mathbf{J}$ is the Jacobian matrix. In this paper, the same transformations from standard element to general element for one-dimensional and two-dimensional basis functions are employed as in Ref. [17].

2.3. Discretization and implementation

Substituting Eq. (11) into Eq. (6), weighting by $W_j(\mathbf{r})$ and then integrating over the spatial solution domain yields

$$\sum_{p=1}^{N_{\mathrm{sol}}} I_p^{m,n}\int_V \Im^{m,n}[\phi_p(\mathbf{r})]W_j(\mathbf{r})\,\mathrm{d}V = \int_V \widetilde{S}^{m,n}(\mathbf{r})W_j(\mathbf{r})\,\mathrm{d}V, \quad j = 1,\ldots,N_{\mathrm{sol}}, \tag{19}$$

where operator $\Im^{m,n}$ is defined as

$$\Im^{m,n} = \mu^{m,n}\frac{\partial}{\partial x} + \eta^{m,n}\frac{\partial}{\partial y} + \xi^{m,n}\frac{\partial}{\partial z} + \tilde{\beta}^{m,n}(\mathbf{r}). \tag{20}$$

Taking $\Im^m[\phi_j(\mathbf{r})]$ as the weight function, we obtain the least square scheme of spectral element method discretization, which forms the following discretized system of linear equations:

$$\mathbf{K}^{m,n}\mathbf{I}^{m,n} = \mathbf{H}^{m,n}, \tag{21a}$$

where the elements of matrix $\mathbf{K}^{m,n}$ and $\mathbf{H}^{m,n}$ are expressed as

$$K_{jp}^{m,n} = \int_V \left(\mu^{m,n}\frac{\partial\phi_p(\mathbf{r})}{\partial x} + \eta^{m,n}\frac{\partial\phi_p(\mathbf{r})}{\partial y} + \xi^{m,n}\frac{\partial\phi_p(\mathbf{r})}{\partial z} + \tilde{\beta}^{m,n}(\mathbf{r})\phi_p(\mathbf{r})\right) \times \left(\mu^{m,n}\frac{\partial\phi_j(\mathbf{r})}{\partial x} + \eta^{m,n}\frac{\partial\phi_j(\mathbf{r})}{\partial y} + \xi^{m,n}\frac{\partial\phi_j(\mathbf{r})}{\partial z} + \tilde{\beta}^{m,n}(\mathbf{r})\phi_j(\mathbf{r})\right)\mathrm{d}V, \tag{22a}$$

$$H_j^{m,n} = \int_V \widetilde{S}^{m,n}(\mathbf{r})\left(\mu^{m,n}\frac{\partial\phi_j(\mathbf{r})}{\partial x} + \eta^{m,n}\frac{\partial\phi_j(\mathbf{r})}{\partial y} + \xi^{m,n}\frac{\partial\phi_j(\mathbf{r})}{\partial z} + \tilde{\beta}^{m,n}(\mathbf{r})\phi_j(\mathbf{r})\right)\mathrm{d}V. \tag{22b}$$

Boundary conditions must be imposed before solving Eq. (21). Here, collocation technique is used to impose the boundary condition given by Eq. (2). For the Dirichlet boundary condition, boundary operator can be considered as an identity operator, and it is an identity matrix in discretized form. To impose the boundary condition, we only need to replace the row of stiff matrix $\mathbf{K}^{m,n}$ with index of boundary node by the corresponding row of identity matrix. At the same time, replace the corresponding row of the vector $\mathbf{H}^{m,n}$ by radiation intensity of the boundary node. Thus for each node j on the inflow boundary of direction m described by Eq. (2), this algorithm can be written as

$$K_{jp}^{m,n} = \begin{cases} 1, & j = p \\ 0, & j \neq p \end{cases}, \tag{23a}$$

$$H_j^{m,n} = I_j^{m,n}. \tag{23b}$$

The discretized linear equation of each direction given in Eq. (21) can be solved by many methods. In this paper, it

was solved by the direct method direction by direction. Because the source term of the discrete-ordinates equation in direction $\mathbf{\Omega}^{m,n}$ contains the radiative intensities of the other directions, global iterations are necessary to update the source term. The implementation of the least square spectral element method can be carried out according to the following routine:

Step 1. Mesh the solution domain with quadrilateral elements.
Step 2. Choose the order of Chebyshev polynomial to build elemental basis function and generate the solution nodes for each element with Gauss–Chebyshev–Lobatto points.
Step 3. Give initial value for radiative intensity and begin the source term update loop.
Step 4. Begin loop each angular direction for $m = 1,\ldots,N_\theta$ and $n = 1,\ldots,N_\varphi$, build the basis function for each element V_e from standard element V_{st}, integrate on each element and then assemble to get global stiff matrix $\mathbf{K}^{m,n}$, and $\mathbf{H}^{m,n}$.
Step 5. Impose boundary condition according to the algorithm described by Eq. (23).
Step 6. Solve the linear equation (21) to get the radiative intensity on each solution nodes for angular direction $\mathbf{\Omega}^{m,n}$, then end angular loop.
Step 7. Terminate the iteration process if the stop criterion is satisfied. Otherwise go back to Step 4.

In this paper, the maximum relative error 10^{-4} of radiative intensity is taken as stopping criterion for iteration.

3. Results and discussion

Based on the formulation described above, a computer code capable of modeling multidimensional radiative transfer problems in a graded index media has been developed. *p*-Convegence characteristics of the least square spectral element method for radiative transfer equation in grade index media are studied. Grid refinement studies were performed for solutions to ensure that the solutions are independent of grid size. In the following discusses about spatial discretization effects, the angular grids are refined enough to ensure that the results are independent of the angular discretization. Five test problems are examined to verify the performance of the method described above. The test cases are selected because exact, or at lease very precise, solutions of the radiative transfer equation exist for comparison with the LSSEM solution. All the computation is executed on a computer with CPU of AMD Athlon 2200 + (1.8 GHz) and 512 M RAM. In order for quantitative comparison between results obtained by LSSEM (denoted as $R_{\mathrm{LSSEM}}(x)$) and the exact or quasi-exact results (denoted as $R_{\mathrm{Exact}}(x)$) in references, the integral averaged relative error is defined as following:

Integral averaged relative error

$$= 100 \times \frac{\int |R_{\mathrm{LSSEM}}(x) - R_{\mathrm{Exact}}(x)|\mathrm{d}x}{\int |R_{\mathrm{Exact}}(x)|\mathrm{d}x} \tag{24}$$

3.1. Case 1: radiative equilibrium in non-scattering media with linear refractive index

The least square spectral element method is applied to a radiative equilibrium problem in a one-dimensional semi-transparent slab bounded by black walls. The temperatures of boundary walls are imposed as $T_0 = 1000$ K and $T_L = 1500$ K at $x = 0$ and $x = L$, respectively. The refractive index of the media within the slab varies linearly with the axis coordinate as $n(x) = 1.2 + 0.6x/L$. The media within the slab is non-scattering. This case has also been used as a test case by Huang et al. [4] using the pseudo source adding method. The temperature distributions within the media are presented in Fig. 1 for three values of slab optical thicknesses, namely, $\tau_L = 0.01$, $\tau_L = 1.0$ and $\tau_L = 3.0$, respectively. Here five elements are used with fourth-order polynomial for space decomposition, and the

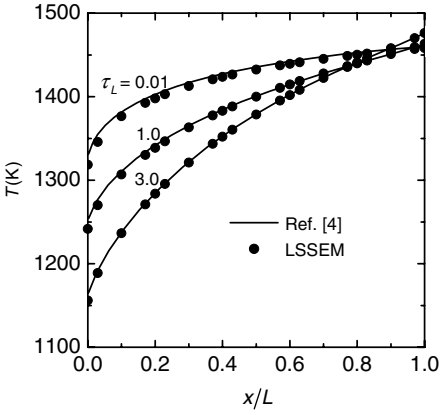

Fig. 1. Temperature distributions in the case of $n(x) = 1.2 + 0.6x/L$, $\varepsilon_0 = \varepsilon_L = 1$ and $\omega = 0$.

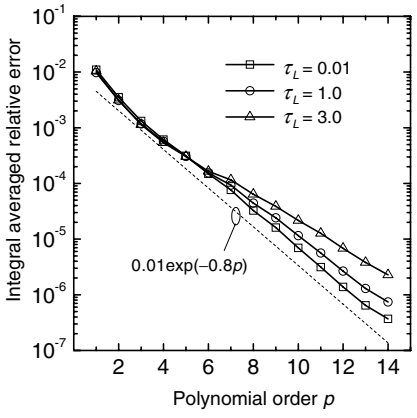

Fig. 2. *p*-Convergence characteristics of LSSEM for solution of temperature distributions between slabs filled with linear refractive index for different optical thickness.

total solid angle is subdivided into $N_\theta = 20$. The computational time are about 2, 5, and 9 s for $\tau_L = 0.01$, 1.0, and 3.0, respectively. As shown in Fig. 1, the LSSEM results are in good agreement with the results obtained by using the pseudo source adding method. The maximum integral averaged relative error based on the data in Ref. [4] is less than 0.8%.

The effects of polynomial order p on the convergence characteristics of the LSSEM in solving the temperature distributions in linear refractive index media for three values of optical thicknesses, namely, $\tau_L = 0.01$, 1.0 and 3.0, are studied, respectively. Here, two spectral elements are used. Because there is no analytical solution, the results obtained by 15 order polynomial are taken as benchmark solutions for comparison. The integral averaged relative errors are plotted in Fig. 2 for various polynomial orders. An exponential decay function, $0.01\exp(-0.8p)$, is also plotted for comparison. As can be seen from Fig. 2, the convergence rate of LSSEM is very fast and approximately follows the exponential law.

3.2. Case 2: radiative equilibrium in non-scattering media with sinusoidal refractive index

In this case, non-linear refractive index is studied. The temperatures of boundary walls are imposed as $T_0 = 1000$ K and $T_L = 1500$ K at $x = 0$ and $x = L$, respectively. The refractive index of media within the slab varies sinusoidally with the axis coordinate as $n(x) = 1.8 - 0.6\sin(\pi x/L)$. The media within the slab is non-scattering and the slab optical thickness is $\tau_L = 1.0$. The least square spectral element method is applied to this case with fourth-order polynomial and five elements for spatial decomposition. Fig. 3 shows the temperature distributions within the media for two different conditions of wall emissivity, namely $\varepsilon_0 = \varepsilon_L = 1$ and $\varepsilon_0 = \varepsilon_L = 0.7$, respectively. As shown in Fig. 3, the LSSEM results are in good agreement with the results obtained by using the pseudo source adding method [21]. The maximum integral averaged relative error is less than 0.4%.

3.3. Case 3: isotropically scattering in a gray enclosure

We consider a square enclosure filled with isotropically scattering gray media. The single scattering albedo of media is $\omega = 1.0$. The lower wall is kept hot, which temperature is denoted as T_{w1}, but all other walls and the media enclosed by the square enclosure are kept cold (0 K). The optical thickness based on the side length $L(L = 0.1$ m) of square enclosure is $\tau_L = (\kappa_a + \kappa_s)L = 0.1$. The media temperature, the absorption coefficient and the scattering coefficient of the media enclosed by the square enclosure is uniform, but the refractive index is a linear function of spatial position as following:

$$n(x, y) = 1 + 2(x + y)/L. \tag{25}$$

As shown in Fig. 4, the square is uniformly discretized into many rectangular elements. The LSSEM is applied to solve the dimensionless net radiative heat fluxes on the lower wall, in which fourth-order polynomial is used. The total angular space is subdivided into $N_\theta \times N_\varphi = 10 \times 21$ control solid angles. The dimensionless net radiative heat

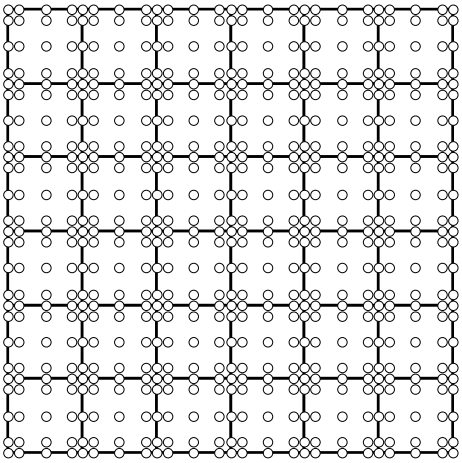

Fig. 4. Uniform decomposition and spectral nodal distribution of square enclosure (with 36 elements).

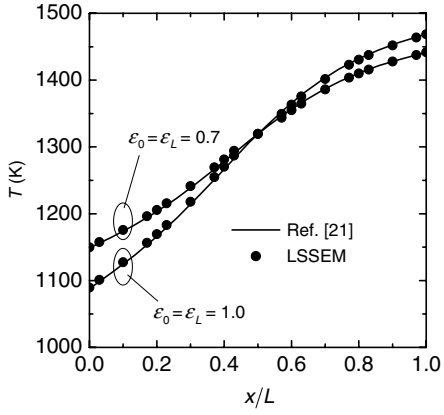

Fig. 3. Temperature distributions in the case of $n(x) = 1.8 - 0.6\sin(\pi x/L)$, $\tau_L = 1$ and $\omega = 0$.

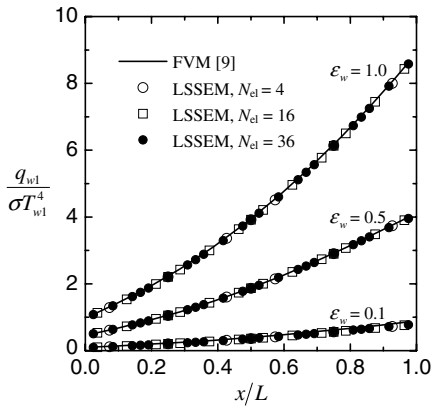

Fig. 5. Dimensionless net wall radiative heat flux on the bottom wall of a gray enclosure filled with a purely scattering media.

fluxes $q_{w1}/\sigma T_{w1}^4$ on the bottom wall are presented in Fig. 5 by using three different spatial decomposition schemes, namely, 4, 16, and 36 elements, and compared to the results obtained from the FVM presented in Ref. [9]. The LSSEM results agree with those of FVM very well. No observable difference could be detected between the results of LSSEM and FVM when they are presented in graphical form. Grid refinement test show that all three decomposition schemes give accurate results, which demonstrate grid size independence of the method. Because of asymmetric distribution of refractive index, the profiles of dimensionless net radiative heat flux are asymmetric, which are different from the case of uniform refractive index [22].

3.4. Case 4: anisotropically scattering in a black enclosure

In this case, the radiative heat transfer in a square enclosure with black walls and an anisotropically scattering media is studied. The side length of square enclosure is $L = 0.1$ m. The media is kept hot, but the temperatures of all the boundary walls are kept as 0 K. In the following analysis, the linear phase function $\Phi(\mathbf{\Omega}', \mathbf{\Omega}) = 1 + \mathbf{\Omega}' \cdot \mathbf{\Omega}$ is used. The media temperature T_g, the absorption coefficient κ_a, and the scattering coefficient κ_s of the media enclosed by the square enclosure is uniform, while the refractive index is a linear function of spatial position the same as in Case 3 (Eq. (25)). The optical thickness based on the side length L of square enclosure is $\tau_L = (\kappa_a + \kappa_s)L = 0.1$.

The LSSEM is applied to this case, in which fourth-order polynomial is used. The total angular space is subdivided into $N_\theta \times N_\varphi = 10 \times 21$ control solid angles. The square enclosure is uniformly decomposed into 36 elements as shown in Fig. 4. The dimensionless net radiative heat fluxes $q_{w1}/\sigma T_g^4$ on the lower wall are shown in Fig. 6 for three different values of single scattering albedo ω, namely 0.0, 0.5 and 0.9, and compared to the results obtained from FVM presented in Ref. [9]. By comparison, it can be seen that the LSSEM presented in this paper has a good accuracy in solving the radiative heat transfer in graded index media with anisotropically scattering. Even in the case of $\omega = 0.0$,

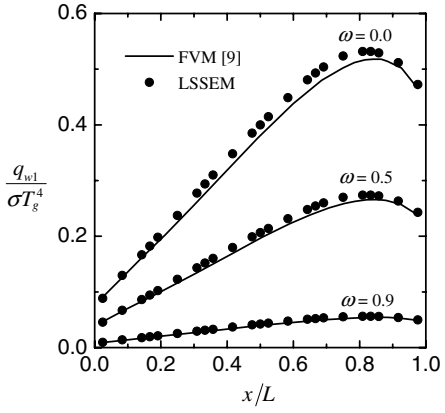

Fig. 6. Dimensionless net wall radiative heat flux on the bottom wall of a black enclosure filled with anisotropically scattering media.

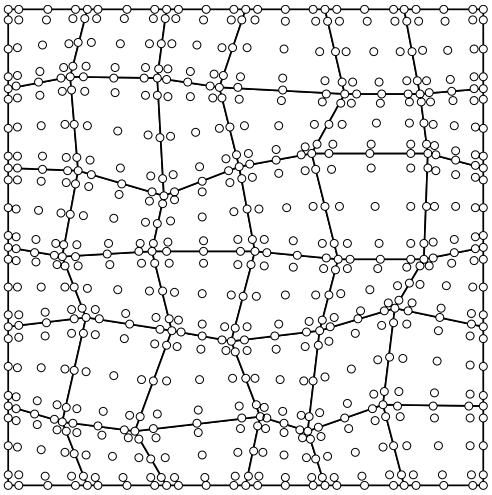

Fig. 7. Non-uniform decomposition and spectral nodal distribution in a square enclosure (with 36 elements).

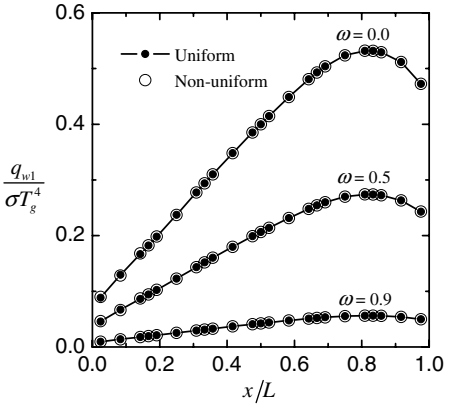

Fig. 8. Comparison of dimensionless net wall radiative heat flux obtained using the uniform and the non-uniform decomposition schemes.

the maximum integral averaged relative error is less than 5%. LSSEM is of p-convergence, and is expected to be more accurate. In FVM, the step scheme is often used for spatial discretization, therefore FVM is of low-order convergence, and the results of FVM suffer from false scattering.

To check the performance of LSSEM on skewed grid, as shown in Fig. 7, a non-uniform decomposition is considered. Fig. 8 shows the dimensionless net radiative heat fluxes $q_{w1}/\sigma T_g^4$ on the lower wall obtained using the uniform and the non-uniform decomposition schemes. It can be seen that the difference of radiative heat flux obtained using the uniform and the non-uniform decomposition schemes is very little. The maximum integral averaged relative difference of these two results based on the solution from uniform grid is less than 0.05%.

3.5. Case 5: anisotropically scattering with non-linear refractive index

We consider radiative heat transfer in a square enclosure with black walls and filled with anisotropically scattering

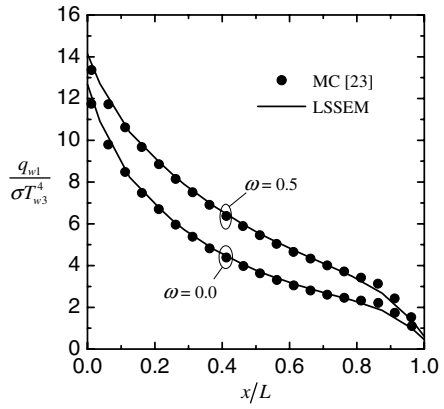

Fig. 9. Dimensionless net wall radiative heat flux on the bottom wall of a black enclosure filled with anisotropically scattering media of non-linear refractive index.

gray media of non-linear refractive index. The temperature of left wall is denoted as T_{w3} and kept as 1000 K, but all other walls and the media enclosed by the square enclosure are kept as 0 K. The optical thickness based on the side length L of square enclosure is $\tau_L = (\kappa_a + \kappa_s)L = 1$. The linear scattering phase function $\Phi(\mathbf{\Omega}', \mathbf{\Omega}) = 1 + \mathbf{\Omega}' \cdot \mathbf{\Omega}$ is used. The media temperature, the absorption coefficient and the scattering coefficient of the media enclosed by the square enclosure is uniform. The refractive index is a function of spatial position as

$$n(x, y) = 5\left[1 - 0.9025\left(\frac{x}{L}\right)^2\right]^{0.5}. \quad (26)$$

LSSEM is applied to solve the dimensionless net radiative heat fluxes on the lower wall for $\omega = 0$ and $\omega = 0.5$, respectively. The square enclosure is divided uniformly into 16 uniform quadrilateral elements and fourth-order polynomial is used for spectral approximation. The total angular space is subdivided into $N_\theta \times N_\varphi = 18 \times 36$ control solid angles. The dimensionless net radiative heat fluxes $q_{w1}/\sigma T_{w3}^4$ on the bottom wall are presented in Fig. 9 and compared to the results obtained from Monte Carlo (MC) simulation in Ref. [23]. It can be seen from Fig. 9 that the LSSEM results agree good with those of MC. The maximum integral averaged relative error is less than 3%. No obvious ray effects and false scattering are observed.

4. Conclusions

To avoid the complicated computation of curved ray tracing, the least square spectral element method based on discrete-ordinate equation is extended to solve multidimensional radiative heat transfer problem in semitransparent graded index media. Chebyshev polynomial is employed as expansion set for the spectral element discretization. The p-convergence characteristics of the least square spectral element method are studied for radiative transfer equation in grade index media. The convergence rate is very fast and approximately follows the exponential law. Five various test problems were taken as examples to verify the least square spectral element formulation. The predicted distributions of temperature and radiative heat flux are determined by the least square spectral element method and compared with data in the references. The results show that the least square spectral element method has good accuracy for solving multidimensional radiative heat transfer problems in semitransparent graded index media.

Acknowledgement

The support of this work by the National Nature Science Foundation of China (50425619, 50336010) is gratefully acknowledged.

References

[1] P.B. Abdallah, V.L. Dez, Thermal field inside an absorbing-emitting semitransparent slab at radiative equilibrium with variable spatial refractive index, J. Quant. Spectrosc. Radiat. Transf. 65 (4) (2000) 595–608.
[2] P.B. Abdallah, V.L. Dez, Thermal emission of a two-dimensional rectangular cavity with spatial affine refractive index, J. Quant. Spectrosc. Radiat. Transf. 66 (6) (2000) 555–569.
[3] P.B. Abdallah, V.L. Dez, Thermal emission of a semi-transparent slab with variable spatial refractive index, J. Quant. Spectrosc. Radiat. Transf. 67 (3) (2000) 185–198.
[4] Y. Huang, X.L. Xia, H.P. Tan, Temperature field of radiative equilibrium in a semitransparent slab with a linear refractive index and gray walls, J. Quant. Spectrosc. Radiat. Transf. 74 (2) (2002) 249–261.
[5] Y. Huang, X.L. Xia, H.P. Tan, Radiative intensity solution and thermal emission analysis of a semitransparent media layer with a sinusoidal refractive index, J. Quant. Spectrosc. Radiat. Transf. 74 (2) (2002) 217–233.
[6] L.H. Liu, Discrete curved ray-tracing method for radiative transfer in an absorbing-emitting semitransparent slab with variable spatial refractive index, J. Quant. Spectrosc. Radiat. Transf. 83 (2) (2004) 223–228.
[7] L.H. Liu, H.C. Zhang, H.P. Tan, Monte carlo discrete curved ray-tracing method for radiative transfer in an absorbing-emitting semitransparent slab with variable spatial refractive index, J. Quant. Spectrosc. Radiat. Transf. 84 (3) (2004) 357–362.
[8] L.H. Liu, Finite volume method for radiation heat transfer in graded index media, J. Thermophys. Heat Transf. 20 (1) (2006) 59–66.
[9] L.H. Liu, L. Zhang, H.P. Tan, Finite element method for radiation heat transfer in multi-dimensional graded index media, J. Quant. Spectrosc. Radiat. Transf. 97 (2006) 436–445.
[10] A.T. Patera, A spectral element method for fluid dynamics – laminar flow in a channel expansion, J. Comp. Phys. 54 (1984) 468–488.
[11] G.E. Karniadakis, S.J. Sherwin, Spectral/hp Element Methods for cfd, Oxford University Press, 1999.
[12] R.D. Henderson, G.E. Karniadakis, Unstructured spectral element methods for simulation of turbulent flows, J. Comp. Phys. 122 (1995) 191–217.
[13] M.O. Deville, P.F. Fischer, E.H. Mund, High-order Methods for Incompressible Fluid Flow, Cambridge University Press, 2002.
[14] C.H. Amon, B.B. Mikic, Spectral element simulations of unsteady forced convective heat transfer. Application to compact heat exchanger geometries, Numer. Heat Transf. A 19 (1) (1991) 1–19.
[15] J.P. Pontaza, J.N. Reddy, Least-squares finite element formulations for one-dimensional radiative transfer, J. Quant. Spectrosc. Radiat. Transf. 95 (3) (2005) 387–406.

[16] J.C. Chai, S.V. Patankar, Finite-volume method for radiation heat transfer, Adv. Numer. Heat Transf. 2 (2000) 109–141.
[17] J.M. Zhao, L.H. Liu, Least square spectral element method for radiative heat transfer in semitransparent media, Numer. Heat Transfer B 50 (2006) 473–489.
[18] J.P. Berrut, L.N. Trefethen, Barycentric Lagrange interpolation, SIAM Rev. 46 (3) (2004) 501–517.
[19] R. Baltensperger, M.R. Trummer, Spectral differencing with a twist, SIAM J. Sci. Comput. 24 (5) (2003) 1465–1487.
[20] N.J. Higham, The numerical stability of barycentric Lagrange interpolation, IMA J. Numer. Anal. 24 (2004) 547–556.
[21] H.P. Tan, Y. Huang, X.L. Xia, Solution of radiative heat transfer in a semitransparent slab with an arbitrary refractive index distribution and diffuse gray boundaries, Int. J. Heat Mass Transf. 46 (11) (2003) 2005–2014.
[22] L.H. Liu, Finite element simulation of radiative heat transfer in absorbing and scattering media, J. Thermophys. Heat Transf. 18 (2004) 555–557.
[23] L.H. Liu, Benchmark numerical solutions for radiative heat transfer in two-dimensional media with graded index distribution, J. Quant. Spectrosc. Radiat. Transf. 102 (2) (2006) 293–303.